ACS APPLIED MATERIALS & INTERFACES

Research Article

www.acsami.org

Preparation and Optimization of Silver Nanoparticles Embedded Electrospun Membrane for Implant Associated Infections Prevention

Heran Wang,[†,‡,§] Ming Cheng,[‡,§,⊥] Jianming Hu,[#] Chenhong Wang,[†,‡] Shanshan Xu,*[,†] and Charles C. Han*[,†]

[†]State Key Laboratory of Polymer Physics and Chemistry, Joint Laboratory of Polymer Science and Materials, Beijing National Laboratory for Molecular Sciences, Institute of Chemistry, Chinese Academy of Sciences, Beijing 100190, China

[‡]University of Chinese Academy of Sciences, Beijing 100049, China

[⊥]Beijing National Laboratory for Molecular Sciences, Key Laboratory of Molecular Nanostructures and Nanotechnology, Institute of Chemistry, Chinese Academy of Sciences, Beijing 100190, China

[#]The First Affiliated Hospital of Soochow University, Suzhou 215000, China

ABSTRACT: A strategy of using silver nanoparticle (AgNP)-loaded electrospun membrane as a novel coating material for preventing implant associated infections is reported. The strategy takes both the advantages of the excellent antibacterial as well as no drug resistance properties of AgNPs, and the widely used biodegradable electrospun membrane to serve as AgNP carrier and physical obstruction of bacteria adhesion. However, AgNPs have not been applied in clinical treatment yet because the concern of the potential toxicity. For the first time, we systematically investigated toxicity of AgNP-based coating materials in vitro and in vivo. Three dosages (0.1, 0.5, and 1.0 wt %) of silver nanoparticles (AgNPs) were embedded in biodegradable PLGA electrospun membranes as treatment devices to determine the precise concentration of AgNPs, minimize the dosage, and consequently reduced the toxicity in clinical applications. On the basis of antibacterial results and toxicity evaluations, PLGA electrospun membranes containing 0.5 wt % of AgNPs was considered as the most suitable combination, which is safe and effective for clinical application.

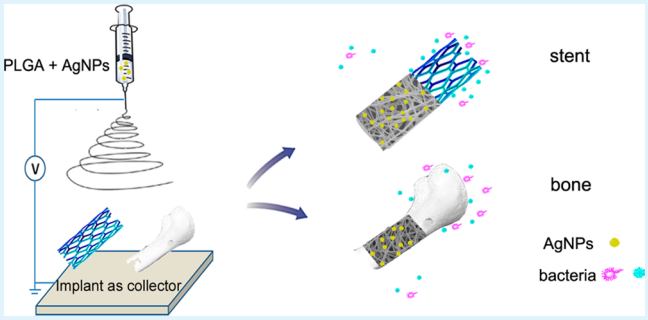

KEYWORDS: *silver nanoparticles, PLGA electrospun nanofibers, implant coating material, antibacterial activity, implant associated infections, biotoxicity*

1. INTRODUCTION

With the worldwide increase in life expectancy and advances in medical technology, the demand for medical implants is growing.[1] However, patients suffer continuing problems of bacterial infection caused by medical implanted devices.[2,3] A huge economic expenditure to society is caused by these kinds of implant-associated infections besides human pain and suffering. This number is more than $3 billion in the United States every year, and will continue to rise as more patients receive biomedical implants. To meet the enormous clinical and marketing requirement, an effective treatment method to prevent or even reduce such infections is definitely needed.

At the cellular level, bacterial adhesion and subsequent biofilm formation lead to infection at the implant location.[4] Generally, a large amount of antibiotics is injected to prevent the infections in clinic. However, the effectiveness of injection or oral administration is far from satisfactory, because the drug is rapidly delivered into systemic circulation, which leads to high adverse effects and low efficacy.[5] Therefore, the most direct approach for improving the therapy efficacy is to deliver antibacterial agents by controllable manner on the surface of the implant.[6] Such implant coatings should release high initial concentration of antibiotic reagents in the crucial short term (hours to one day) to obstruct the initial bacteria adhesion and long-term release (weeks to months) to prevent the formation of fibrous capsule and tissue integration. Among all the coating materials, PLGA electrospun fibrous membranes could be an appropriate delivery platform, which has all the essential properties for implant coating materials, such as admirable biocompatibility,[7,8] easy attachment to the surface of all implants,[9] controllable drug release profile by adjusting the composition of the fibers.[10,11] Moreover, it has been reported that PLGA electrospun fibers have excellent antiadhesion property,[12] which could reduce surface colonization and prevent the formation of biofilms.

The most common pathogens that cause implant infections include Gram-positive *Staphylococcus aureus* and Gram-negative *Escherichia coli*.[13] According to the recent research, these

Received: August 6, 2013
Accepted: October 11, 2013
Published: October 11, 2013

bacterial strains have the protective polysaccharide coating and sequestered nutrients, thus exhibit extreme resistance to most antibiotics.[14] However, silver nanoparticles (AgNPs) possess a high antimicrobial effectiveness against these pathogens and will not develop drug resistance.[15−17] Since the toxicity of AgNPs to normal cells or human has not been fully evaluated yet, the widespread concern limited the application of AgNPs as a clinical antibacterial agent.[18,19] Therefore, a study on the cytotoxicity of AgNPs would be particularly needed.

Here, we designed and prepared an AgNP-loaded electrospun membrane, an antimicrobial coating platform that could directly spin and attach on the surface of implants by adjusting the electronic field and meanwhile rotating the implants.[20,21] Our platform takes the advantages of both the excellent antibacterial properties of AgNPs and the widely used PLGA electrospun membrane to serve as delivery carrier and prevent initial bacteria adhesion. (Scheme 1) Different dosages of AgNPs were embedded in electrospun membranes and the release profiles were measured. To determine the precise concentration of AgNPs to inhibit infection and thus reduce the toxicity in clinical applications, we investigated the antimicrobial activity of electrospun membranes with different AgNP doses. Subsequently, the dose−effect of AgNPs on cell viability and in vivo acute toxicity were systematically evaluated to optimize the concentration of AgNPs loaded in electrospun membrane. We hypothesize that this approach could provide a safe, effective, and feasible coating platform to resist implant-associated infections.

Scheme 1. Schematic Illustration of the Antibacterial Effect of AgNPs Carrying Electrospun Fibrous Membrane on the Stent and Bone

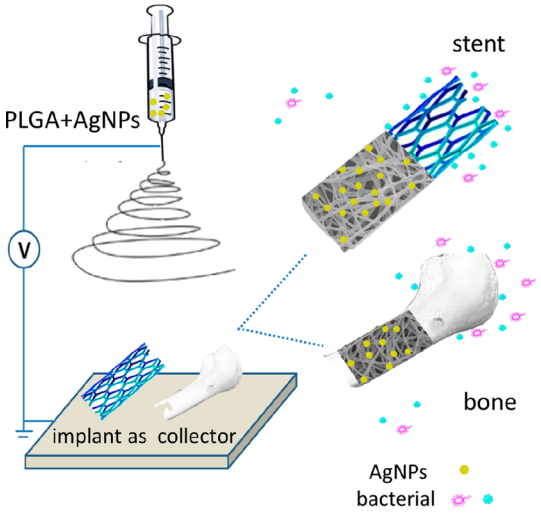

2. EXPERIMENTAL SECTION

2.1. Preparation of AgNPs and AgNP-Loaded Electrospun Membranes. *2.1.1. Preparation of AgNPs.* Procedures for the preparation of polyvinylpyrrolidone (PVP) stabilized monodispersed AgNPs were prepared as described in the literature before.[22] In brief, 10% (w/v) PVP(M_w = 55 000 g/mol, Aldrich)/ethylene glycol solution (20 mL) was prepared under stirring and heating (180 °C) for 0.5 h. Subsequently, 10 mL of $AgNO_3$/ethylene glycol (2%, w/v) solution was slowly added to the PVP solution under 140 °C. After stirring for 15 min of the reaction, we cooled the mixed solution to 20 °C. The AgNPs were obtained by precipitated with surplus acetone and five times centrifugation and washing.

2.1.2. Preparation of AgNP-Loaded Electrospun Membranes. Poly(D,L-lactic-co-glycolic acid) (PLGA, molar ration of lactide-to-glycolide =75/25, M_w = 60 000 g/mol) was obtained from Daigang Biological Technology Co. Ltd. (Jinan, China). The AgNPs were added into the 50 w/v% PLGA solution ($V_{DMF}/V_{acetone}$ = 1/1) and concentrations were varied from 0.1, 0.5, to 1.0 wt %. The nanofibers were prepared by a normal electrospinning equipment with 10-jets and a rotating drum. The fibrous membranes were 100 ± 10 μm thickness after 40 min collection, and then put in a vacuum for 7 days to fully remove the solvent.

2.2. Characterization. *2.2.1. AgNP Size Measurements.* The size of AgNPs was characterized by transmission scanning electron microscope (TEM, JEM-2200, Japan) and atomic force microscopy (AFM, N9524A-US08380108, USA). And the size distribution of AgNPs was measured by dynamic light scattering (DLS, NanoV510, Malvern, UK).

2.2.2. Characterization of Electrospun Membranes. The morphologies of the AgNP-loaded membranes were investigated by TEM and scanning electron microscope (SEM, JEOL JSM- 6700F, Japan). The mean fiber diameter of electrospun membranes were calculated by Nano Measure software. Static contact angle of distilled water on the surface of the membranes was measured and the value was an average of 5 independent measurements. High-resolution X-ray photoelectron spectroscopy (XPS) was chosen to study the surface chemical composition of the fibers. The data was measured by ESCALab220i-XL electron spectrometer using 300 W AlKα radiation and the analyzer angle to the sample's surface was 90°.

2.3. In Vitro Silver Release. The released amount of silver from electrospun membranes was analyzed by Inductively Coupled Plasma Mass Spectrometry (ICP-MS, Thermo-Fisher). Samples were cut into 5 × 5 cm^2 pieces. After weighted, the specimen was put into a centrifugation tube with 10 mL of phosphate-buffered saline (PBS, pH 7.4), and then put the tubes in a 37 °C incubator for 1 week. Two and a half milliliters of released solution was extracted from the solution at different time intervals, and then added back 2.5 mL of fresh PBS to keep the total amount. To determine the encapsulation efficiency, samples were dissolved in 1 mL aqua regia at the seventh day, and then diluted for ICP-MS analysis. All experiments were repeated three times, and the data are reported in the form of average ± SD.

2.4. In Vitro Antibacterial Activity Assay. *Staphylococcus aureus* (Gram-positive, ATCC 25923) and *Escherichia coli* (Gram-negative; ATCC 25922) were cultivated with Luria−Bertani (LB) broth in sterile tubes. All the membranes containing AgNPs or not were sterilized and cut into size of 2.0 × 2.0 cm^2, and then put into the LB broth with 1 × 10^5 colony forming units of microorganisms. After being shaken at 37 °C for 12 h, the bacteria were collected and cultured on LB agar for another 24 h. Bacterial inhibition rate was determined by counting the bacterial colonies on the agar.

Inhibition zone test was performed on LB solid agar. The membranes (1.0 × 1.0 cm^2) and were placed on bacterial cultured agar, and then incubated at 37 °C for 1 day. The inhibition zone was measured for each sample.

2.5. Cytocompatibility of AgNP-Loaded Electrospun Membranes. *2.5.1. Cell Culture.* NIH/3T3 fibroblasts came from ATCC Cell Biology Collection. Cells were seeded in DMEM (Gibco) with 4.5 g/L glucose supplemented with 10% FBS (Hyclone), 0.5% PenStrep (Invitrogen) in a cell incubator at 37 °C in 5% CO_2.

2.5.2. Confocal Laser Scanning Imaging. NIH/3T3 fibroblasts were seeded in culture plates. After the cells were adherent to the culture dish, AgNP-loaded electrospun membranes (2.0 × 2.0 cm^2) were induced to the culture medium (1 mL). The cells without treated by electrospun membranes were served as controls. Twenty-four hours later, the cells were washed with PBS for three times, and then fixed in cold 4% paraformaldehyde/PBS solution for 15 min, followed by permeabilized in PBS containing 0.5% Triton X-100 solution. Propidium iodide (PI), a cell nonpermeable red fluorescent dye (Ex/Em = 488/615), was used to stain dead cells. The steps of staining trials came from instruction to the product. An epi-fluorescence microscope was used to image the stained cells. The actin cytoskeleton in cells was labeled with 300 nM Alexa488-labeled phalloidine

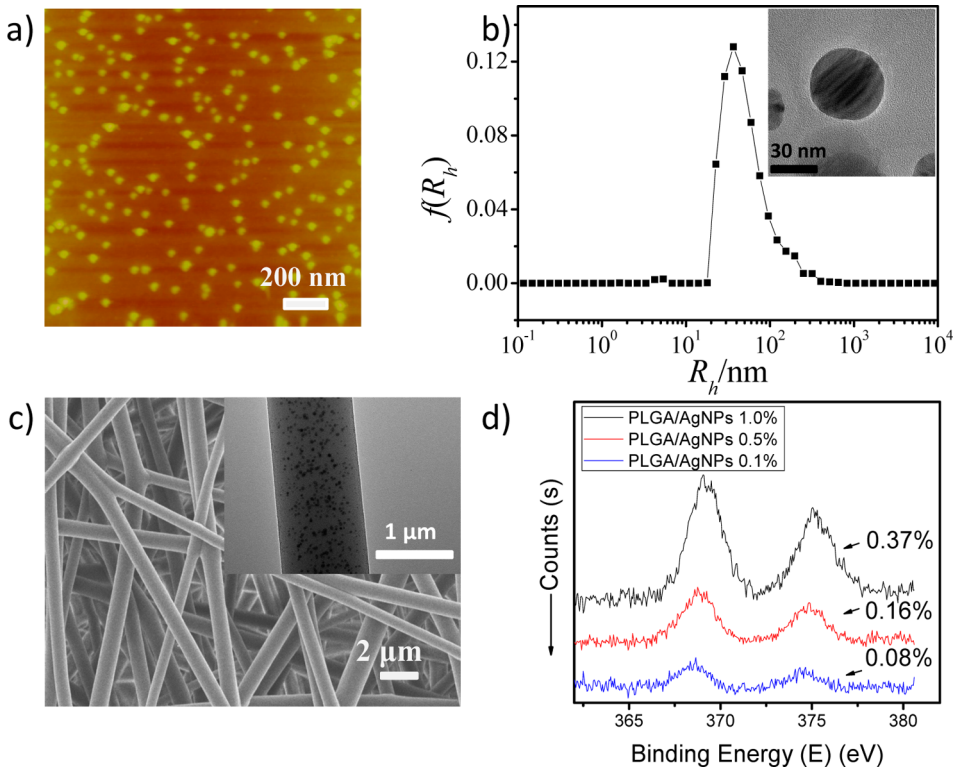

Figure 1. Characterization of AgNPs and AgNP-loaded electrospun membranes. (a) AFM image of AgNPs. (b) AgNP size distribution histograms analyzed by dynamic light scattering (DLS). Inset shows the TEM image of released AgNPs from the membrane. (c) SEM image of the AgNP-loaded electrospun membranes (PLGA/AgNPs 0.5%). Inset shows the TEM image of the AgNP-loaded fiber. (d) XPS spectra of PLGA electrospun membranes with different concentration of AgNPs (0.1, 0.5, and 1.0%).

(Invitrogen, USA) for 30 min and the nuclear was labeled with 1 uM DAPI. Cells were then washed three times in PBS and observed under a confocal microscope (FluoView FV1000, Olympus, USA) with excitation at 405 and 488 nm.

2.5.3. Flow Cytometry Analysis. The cells were rinsed with PBS and then harvested with trypsin, and 2×10^5 cells were then stained and counted using a Dead cell apoptosis Kit with Annexin V Alexa Fluor 488 & PI for Flow Cytometry (V13241, Invitrogen, USA), used as directed. Cells stained for the two markers were measured on an Accuri C6 flow cytometer. The data were analyzed using the CFlow software.

2.6. In Vivo Acute Toxicity. *2.6.1. Animals.* A total of 70 Imprinting Control Region (ICR) mice aged 6−8 weeks (20 ± 1 g) were used as recipients. All animals were provided by the Laboratory of Experimental Animals of the Chinese Academy of Medical Sciences, and all the experiments were performed in accordance with the National Institutes of Health Guide for the Care and Use of Laboratory Animals. Mice were starved overnight before the treatment and they were separated into six experimental groups and one control group. Each group contained five male mice and five female mice. Various concentrations of AgNPs were chosen (6, 7.5, 9, 12, and 15 mg/kg) and the intraperitoneal inject volume was 1 mL. Mice of negative control group were injected with commercial AgNPs (6 mg/kg, negative group). For control subjects, mice were injected with phosphate buffered saline solution. The vital signs, weights, and survival rates were investigated for every group. After 14 days, the mice were sacrificed, and the weight of their organs and their total weight were measured.

2.6.2. Silver Content Analysis. The tissues were added to 3 mL of nitric acid, 0.25 mL of hydrofluoric acid, and 0.5 mL of H_2O_2, and then heated at 200 °C for digestion. Silver contents of organs, blood, and peritoneal lavage fluid were analyzed by ICP-MS.

2.7. Statistical Analysis. The survival rate was calculated by the percent of the rats that was survival during the experiment. All data were presented as mean ± SD. Statistics differences were checked by *t* test, and *p* values <0.05 were considered to be significant.

3. RESULT AND DISCUSSION

3.1. Synthesis and Characterization of AgNP and AgNP-Loaded Electrospun Membranes. AgNPs were synthesized by a previously reported method.[22] Figure 1a depicted the morphologies and Figure 1b showed the size distribution of AgNPs. Via accounting AgNPs from AFM (Figure 1a) images, the size of the products was statistic calculated as about 40 nm. Additionally, the size distribution of AgNPs was determined by DLS. As shown in Figure 1b, AgNPs mean hydrodynamic radius (R_h) was about 46.7 nm, in agreement with the data obtained by AFM. These results suggested that AgNPs were narrowly dispersed and qualified for the following research. Moreover, TEM image of the released AgNPs from the membrane was the same as the synthesized AgNPs, which could verify the electrospun process will not affect the morphology of AgNPs (inset of Figure 1b).

The morphology of AgNP-loaded electrospun membranes was shown in Figure 1c, which were observed to be smooth and bead-free. The embedded rates of AgNPs in all groups were more than 89% by calculation. The mean fiber diameters were 1.11, 0.98, 0.85, and 0.81 μm for electrospun membranes of PLGA/AgNPs 0, 0.1, 0.5, and 1.0%, respectively. The diameter decreased with the increasing amount of AgNPs added into the spinning solution, which is consistent with previous study by Zeng et al.[23] The addition of conductive material could decrease the diameter and narrow the diameter distribution of the fibers because the additives could promote the conductivity and polarizability of the solution. However, the influence of

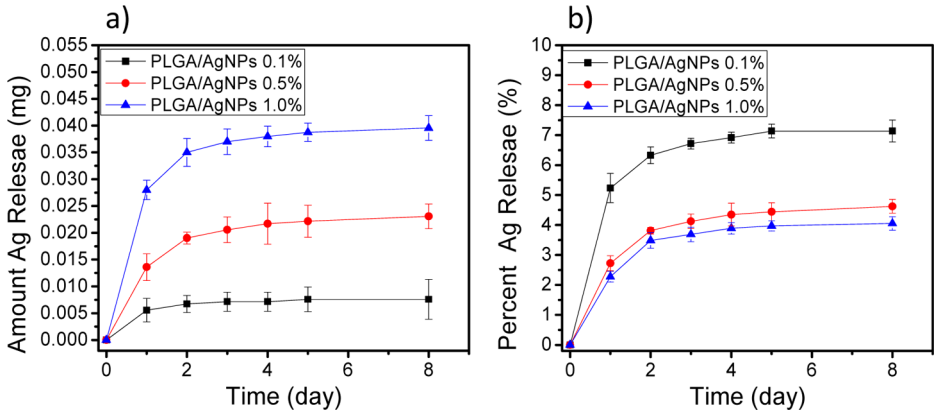

Figure 2. In vitro release profiles of (a) Ag release amount and (b) Ag release percent from electrospun scaffolds.

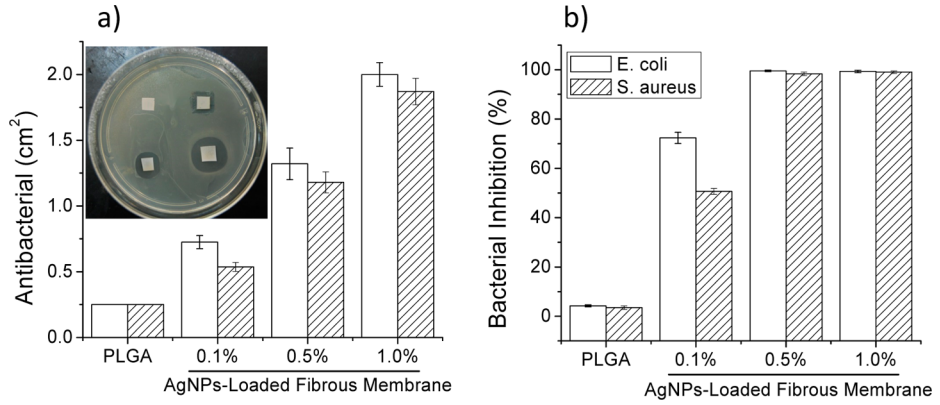

Figure 3. Results of the antibacterial (a) and bacterial inhibition (b) of AgNP-loaded electrospun membranes against *Staphylococcus aureus* and *Escherichia coli*. The inset of a shows the photo of inhibition zone of *Escherichia coli*.

AgNP concentration on the diameter does not affect the dense and smooth structure of the fibers, which indicated that all membranes produced were qualified to be used for the following studies. The contact angles of electrospun membranes were related to the surface structure. We found all the contact angles of membrane were above 120°.[12] This phenomenon indicates that the PLGA electrospun membranes exhibited a highly hydrophobic surface, which could decelerate the contact and leaking of the AgNPs in PBS solution and be helpful to the controlling of AgNP release.

The amount of AgNPs on the electrospun fibers surface was quantified by XPS, which could detect several nanometers depth of the fibers. As shown in Figure 1d, the Ag3d5 spectroscopy varied with the loading amount of AgNPs. Silver content were 0.08, 0.16, and 0.37% by detection on the surface layer of 0.1, 0.5, and1.0% PLGA/AgNP samples, respectively. These quantitative results suggest that fewer AgNPs existed on the surface layer than the inside, which is consistent with the TEM images (inset of Figure 1c). An explanation is the high positive voltage during electrospinning process could affect the distribution of AgNPs to be easily located inside the fibers because of charge repelling effect.[24] Notably, the increase of surface content of silver (1:2:4.6) was not in direct proportion to the increase in AgNP concentration that was dispersed into the polymer solution (1:5:10). With the concentration of AgNPs increased, the ratio of silver on the surface to silver inside decreased. We further discuss this point in combination with the results of silver release from electrospun membranes in the following section.

3.2. Release of AgNPs from PLGA Electrospun Membranes. The release profiles of AgNPs from PLGA membranes are shown in Figure 2. It is clear that all the membranes exhibit an obvious initial burst release. Within the first 24 h, silver released quickly (release percentage >85% to the total release in 7 days) and then released at a slower speed within the successive 6 days. Interestingly, at the first 24 h, the release amount of silver from PLGA/AgNPs 0.1, 0.5, and1.0% membranes were 5.57, 13.6, and 28 μg (1:2.4:5), which is consistent with the surface content proportion of silver analyzed by XPS (1:2:4.6). Therefore, the initial burst release may due to the diffusion of AgNPs nearby the surface layer of the fibers. The possible mechanisms of this phenomenon have been detailed discussed in our previous study.[12] The surface of fibers formed a "skin" that could restrain the internal AgNPs' contact with the solution and release. This could further produce the effect that the AgNPs close to the surface of fibers diffused and been released quickly, while the remaining AgNPs will sustain the slow release along with the degradation of the fibrous membrane.

3.3. ANTIBACTERIAL ACTIVITY

The antibacterial property of the AgNP-loaded membranes was examined against *Staphylococcus aureus* and *Escherichia coli* by zone of inhibition test. Figure 3a shows the inhibition zone of AgNP-loaded electrospun membranes. An inhibition zone, an area showing no antibacterial activity, was not formed around the membranes without AgNPs. However, the AgNP-loaded membranes showed a fair-sized inhibition zone where the

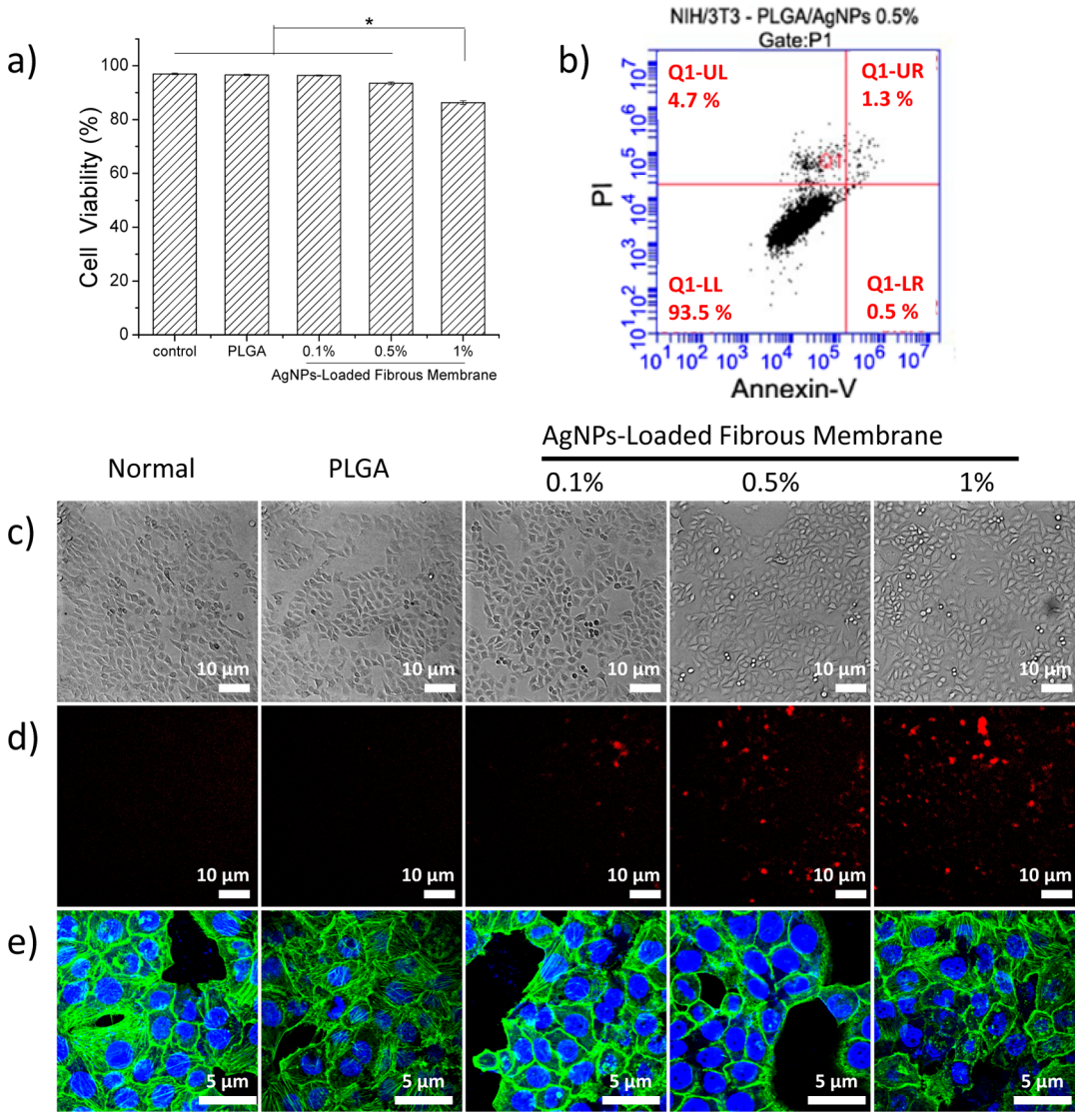

Figure 4. (a, b) Flow cytometry results of Annexin-V and PI double stained samples for NIH/3T3 cells after treated. (c) Cell growth morphology observed by bright field microscope imaging. (d) Wide field fluorescence imaging of the cells after PI stained. (e) Laser scanning confocal imaging after phalloidine and DAPI stained.

bacteria did not proliferate. The size of the inhibition zone varied with the concentration of AgNPs. The more AgNPs loaded, the larger the inhibition zone became. These results are correlated with the release profile of membranes and revealed that the AgNPs, not the PLGA membrane, are the root cause for the antibacterial activity.

To further confirm the bactericidal or bacteriostatic effects, we performed a quantitative method. As can be seen in Figure 3b, the membranes without AgNPs did not present antimicrobial activity (<5%), whereas the proliferation inhibition of bacteria was greatly promoted with the increasing concentration of AgNPs from electrospun membranes. PLGA/AgNPs 0.1% showed 72.3% proliferation inhibition to *Escherichia coli* and 50.6% to *Staphylococcus aureus*, and the proliferation inhibitions by PLGA/AgNPs 0.5% and PLGA/AgNPs 1.0% were all above 99% for both the bacteria. According to the previous study, AgNPs have a special antibacterial mechanism, which could enter the negative charged bacterial cell membrane, react with macromolecular compounds including S, P element (such as nucleic acids, RNA and DNA), and inhibit bacterial replication, resulting in bacteria death;[25] Kim et al. also confirmed that the AgNPs could form free radicals which can attack the liposome membrane by electron spin resonance spectra, resulting in destruction of the cell membrane function.[15] Therefore, the AgNPs could not only destroy bacteria but also kill fungi, mold and spores, which is a huge advantage compared with the commonly used antibiotics. Consequently, we concluded that PLGA/AgNPs 0.5% was the better choice for clinical infection prevention, which could reach 99% antibacterial activity with low AgNP concentration.

3.4. Cytocompatibility Assay. To evaluate the biotoxicity of the AgNPs in the electrospun membrane in vitro, we examined the viability and cellular morphology of cells. NIH/3T3 cells were incubated with blank membrane, 0.1, 0.5, and 1.0% AgNP-loaded membrane, respectively. Twenty-four hours later, cell death was quantified by flow cytometry with Annexin-V and PI double staining. As shown in panels a and b in Figure 4, low cytotoxicity was shown even in 1.0% AgNP-loaded membrane groups (86% alive). To visually assess the cell

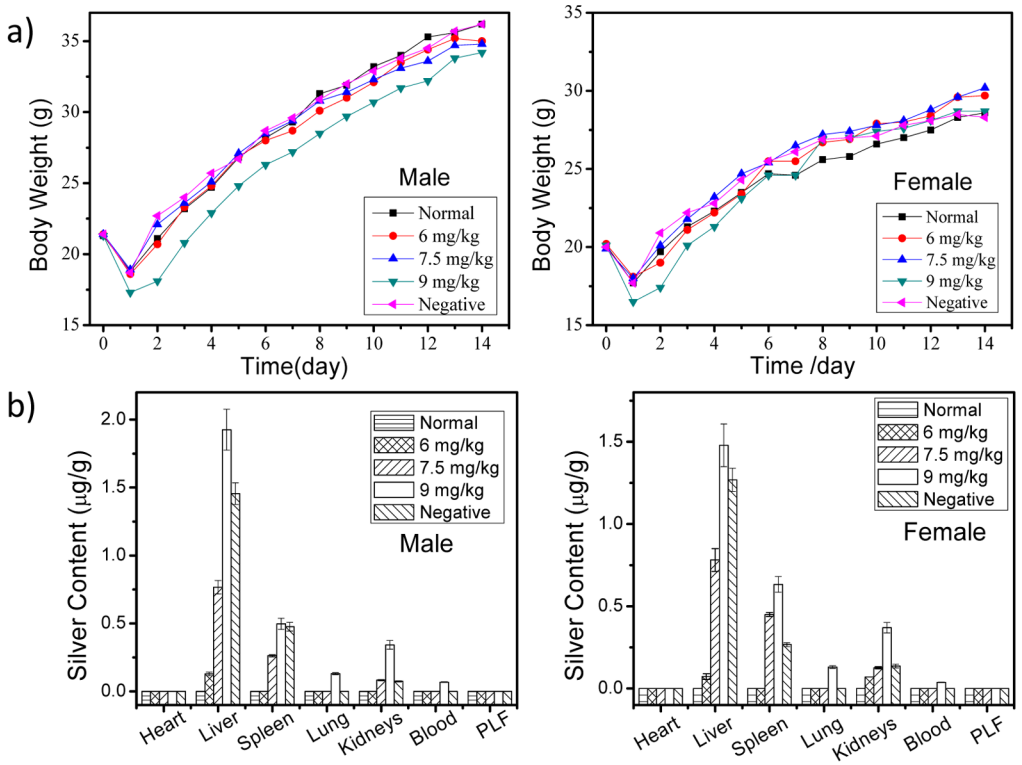

c) **The body weight and coefficients of various tissues to body weight**

		Organ coefficients (mg/g)				
Group	**Body weight (g)**	**Heart**	**Liver**	**Spleen**	**Lung**	**Kidneys**
Male						
Normal	36.1 ± 2.8	5.2 ± 0.1	60.4 ± 3.4	3.6 ± 0.6	6.0 ± 0.6	15.3 ± 0.2
6 mg/kg	35.5 ± 2.3	5.2 ± 1.0	54.7 ± 2.5	5.0 ± 0.7	5.8 ± 0.3	13.8 ± 1.0
7.5 mg/kg	30.0 ± 4.4	6.0 ± 0.8	57.5 ± 6.8	5.1 ± 0.8	6.9 ± 0.4	14.7 ± 2.7
9 mg/kg	32.2 ± 2.1	5.0 ± 0.4	65.1 ± 6.2	6.4 ± 0.6*	6.2 ± 0.4	13.8 ± 0.2
Negative	34.9 ± 3.9	5.1 ± 0.4	52.6 ± 0.8	5.4 ± 0.3	6.1 ± 0.1	13.7 ± 0.6
Female						
Normal	28.0 ± 1.7	5.7 ± 0.8	53.8 ± 2.5	4.5 ± 0.2	6.9 ± 0.1	12.2 ± 0.5
6 mg/kg	28.3 ± 1.5	5.5 ± 0.3	50.9 ± 1.6	5.3 ± 1.2	6.5 ± 0.2	11.9 ± 0.6
7.5 mg/kg	29.4 ± 1.0	4.9 ± 0.2	50.6 ± 1.7	5.9 ± 0.4*	6.5 ± 0.4	12.4 ± 0.3
9 mg/kg	28.6 ± 1.1	4.4 ± 0.4	52.2 ± 7.4	6.8 ± 1.5*	6.9 ± 0.7	13.6 ± 1.9
Negative	28.8 ± 3.2	4.7 ± 0.4	54.9 ± 4.4	5.5 ± 1.0	6.3 ± 0.1	12.3 ± 0.8

Figure 5. (a) Body weight from 1 to 14 days and (b) content of silver in heart, liver, spleen, lung, kidneys, blood, and PLF of mice at 14 days after exposure to different dosages of AgNPs. (c) Body weight and coefficients of various tissues to body weight.

viability, we imaged cells by a wide field microscope with PI staining (Figure 4c, d). Cells in five groups showed minor fluorescence signals, which were consistent with the flow cytometry results. To further evaluate the effect on cellular structure, we labeled the actin cytoskeleton with phalloidin and the nuclear was stained with DAPI, which were observed by confocal microscopy in fixed cells. As shown in Figure 4e, cells that were incubated with AgNP-loaded membranes showed

similar cell morphologies to control cells. On the basis of these results, we determined that the AgNPs at a concentration ≤1%, as used in our electrospinning processes, showed no hazard and did not affect the cellular growth.

3.5. In Vivo Acute Toxicity of AgNPs. To apply AgNPs to human, an acute toxicity test is usually required. As the total amount of AgNPs that loaded in the electrospun membranes were very low and released less than 10% for 7 days, it was difficult to obtain the actual acute toxicity of AgNP-loaded electrospun membranes and the metabolic pathways of AgNPs because of the limitation on the sensitivity of the detection method. Therefore, we reported only the conventional acute toxicity test of drugs to evaluate the in vivo toxicity of AgNPs. Generally, median lethal dose (LD_{50}) is the most important indicator of acute toxicity. In addition, vital signs, body weight changes, and pathological examination are valuable information.[26] Here, the acute toxicity of AgNPs was evaluated with ICR mice.

3.5.1. Vital Signs and Mortality. The mortality was observed and recorded carefully. The large doses (12 and 15 mg/kg) cause convulsions and shock immediately, and all the mice were dead in 10−30 min. In the group of 9 mg/kg, one male and three female mice dead in the first 12 h, the others were alive in the following 14 days. In the low dosage group (6 and 7.5 mg/kg), all the mice survived successfully. Consequently, we calculated the LD_{50} of AgNPs for mice was 8.6 mg/kg.

The symptoms of exposed and survived mice were recorded.[27,28] Compared with the control group, the experimental mice performed remarked loss of appetite and passive behavior after the first two days exposure (Figure 5a). However, the signs of low dosage group (6 and 7.5 mg/kg) gradually disappeared thereafter, whereas high-dose mice (9 mg/kg) still lacked of skin luster and lost body-weight.

3.5.2. Effect of AgNP Concentration to Tissue Injury. The mice were sacrificed 14 days postsurgery. The body weight from 1 to 14 days and coefficients for the heart, liver, spleen, lung, and kidneys to body weights are shown in panels a and c in Figure 5. In all defected groups, there were no differences in the body weight compared with control group. There were no significant changes in heart, liver, lung, and kidney coefficients in all groups. However, the coefficient of spleen was significantly increased in 9 mg/kg group in both that male and female groups ($p < 0.05$), which is consistent with the following silver accumulation tests. The increased spleen coefficient indicated that more toxicity had been induced by AgNPs in the 9 mg/kg group.

3.5.3. Silver Content. The amounts of silver in every organ (heart, liver, spleen, lung, and kidneys), blood, and PLF of mice at 14 days following different exposure dosages of AgNPs are shown in Figure 5b. As can be seen, liver and spleen contained the most AgNPs after treatment and all experimental groups possess a dose-dependent relationship, which means silver accumulated more with increasing injected dosage. In all the organs, liver had the highest silver accumulation. In the 9 mg/kg group, the silver concentration reached 1.93 ± 0.15 μg/g in the male group. Comparatively, silver accumulated in low-dose mice (6 mg/kg) represented no significant difference compared to the control group, which is consistent with the data of 6 mg/kg liver coefficients. Silver also accumulated in spleen, lung, and kidneys (except heart) to various degrees. In spleen for the 9 mg/kg group silver, the content was 0.50 ± 0.04 μg/g, whereas the 6 mg/kg group had no significant difference compared to the control group. In heart tissue, blood, and PLF, no statistics difference in silver content between the experimental and the control group. All the data have the same tendency in the female groups. Consequently, the 6 mg/kg AgNP group showed no toxicity compared to the control group, the concentration lower than 6 mg/kg could be regarded as a safe concentration.

In the previous sections, we suggested that PLGA/AgNPs 0.5% (release 0.092 mg silver from 10 × 10 cm^2 membrane for seven days, 1.5 × 10^{-3} mg/kg in adults) is a proper concentration of AgNPs, which can remarkably inhibit the growth of bacteria with low cytotoxicity. According to the acute toxicity test, this concentration is far lower than 6 mg/kg, which should not accumulate in tissues and should have no influence to the organ coefficient. And this concentration of AgNPs is 3 orders of magnitude lower than LD_{50} for mice, which promises the safety of AgNPs in clinical applications.

4. CONCLUSIONS

In summary, we have designed and prepared a new coating material to prevent implant associated infections, an electrospun PLGA fibrous membrane loaded with AgNPs. In this platform, the polymer membrane served as both the carrier for AgNPs and the coating of implant, providing excellent biocompatibility, controllability of AgNPs in situ release to obtain an initial burst and a long-term release. Our results showed that AgNPs released from the membrane could remain functional after the electrospinning process and had strong antibacterial activity at low AgNP concentration. In addition, it revealed that the antibacterial and biocompatibility of AgNP-loaded membranes were silver-concentration dependent. Because of the concern of the potential toxicity, for the first time, we systematically investigated the toxicity of AgNP-based coating materials in vitro and in vivo. Comprehensive consideration of effectiveness and toxicity, PLGA electrospun membranes containing 0.5 wt% AgNPs was considered as the most suitable combination for clinical applications. We believe this AgNP-loaded electrospun membrane has the capability to reduce the infection rate with no toxicity, which makes it a promising therapeutic coating material for clinical prevention of implant associated infections.

AUTHOR INFORMATION

Corresponding Author

*E-mail: c.c.han@iccas.ac.cn. Tel: +86 10 82618089. Fax: +86 10 62521519.

Author Contributions

§Authors H.W. and M.C. contributed equally. The manuscript was written through contributions of all authors. All authors have given approval to the final version of the manuscript.

Notes

The authors declare no competing financial interest.

ACKNOWLEDGMENTS

This work was financially supported by the National Nature Science Foundation of China (51003110) and the Knowledge Innovation Program of the Chinese Academy of Sciences (Grant KJCX2-YW-H19).

REFERENCES

(1) Hetrick, E. M.; Schoenfisch, M. H. *Chem. Soc. Rev.* **2006**, *35*, 780−789.

(2) Darouiche, R. O. *N. Engl. J. Med.* **2004**, *350*, 1422−1429.

(3) Nablo, B. J.; Prichard, H. L.; Butler, R. D.; Klitzman, B.; Schoenfisch, M. H. *Biomaterials* **2005**, *26*, 6984−6990.
(4) An, Y. H.; Friedman, R. J. *Handbook of Bacterial Adhesion: Principles, Methods, And Applications*; Humana Press: Totowa, NJ, 2000; p 73−90.
(5) Ho, V. P.; Barie, P. S.; Stein, S. L.; Trencheva, K.; Milsom, J. W.; Lee, S. W.; Sonoda, T. *Surg Infect* **2011**, *12*, 255−260.
(6) Wu, P.; Grainger, D. W. *Biomaterials* **2006**, *27*, 2450−2467.
(7) Zong, X.; Li, S.; Chen, E.; Garlick, B.; Kim, K.-s.; Fang, D.; Chiu, J.; Zimmerman, T.; Brathwaite, C.; Hsiao, B. S. *Ann. Surg.* **2004**, *240*, 910−915.
(8) Luu, Y.; Kim, K.; Hsiao, B.; Chu, B.; Hadjiargyrou, M. *J. Controlled Release* **2003**, *89*, 341−353.
(9) Yang, Y.; Xia, T.; Zhi, W.; Wei, L.; Weng, J.; Zhang, C.; Li, X. *Biomaterials* **2011**, *32*, 4243−4254.
(10) Kim, K.; Luu, Y. K.; Chang, C.; Fang, D.; Hsiao, B. S.; Chu, B.; Hadjiargyrou, M. *J. Controlled Release* **2004**, *98*, 47−56.
(11) Maretschek, S.; Greiner, A.; Kissel, T. *J. Controlled Release* **2008**, *127*, 180−187.
(12) Wang, H.; Li, M.; Hu, J.; Wang, C.; Xu, S.; Han, C. C. *Biomacromolecules* **2013**, *14*, 954−961.
(13) An, Y.; Friedman, R. *J. Hosp. Infect.* **1996**, *33*, 93−108.
(14) Smith, A. W. *Adv. Drug Delivery Rev.* **2005**, *57*, 1539−1550.
(15) Kim, J. S.; Kuk, E.; Yu, K. N.; Kim, J.-H.; Park, S. J.; Lee, H. J.; Kim, S. H.; Park, Y. K.; Park, Y. H.; Hwang, C.-Y. *Nanomed.: Nanotechnol. Biol. Med.* **2007**, *3*, 95−101.
(16) Sondi, I.; Goia, D. V.; Matijević, E. *J. Colloid Interface Sci.* **2003**, *260*, 75−81.
(17) Kvítek, L.; Panáček, A.; Soukupová, J.; Kolář, M.; Večerová, R.; Prucek, R.; Holecová, M.; Zboril, R. *J. Phys. Chem. C* **2008**, *112*, 5825−5834.
(18) Nanda, A.; Saravanan, M. *Nanomed.: Nanotechnol. Biol. Med.* **2009**, *5*, 452−456.
(19) Zhang, Y.; Peng, H.; Huang, W.; Zhou, Y.; Yan, D. *J. Colloid Interface Sci.* **2008**, *325*, 371−376.
(20) Katta, P.; Alessandro, M.; Ramsier, R.; Chase, G. *Nano Lett.* **2004**, *4*, 2215−2218.
(21) Li, D.; Xia, Y. *Adv. Mater.* **2004**, *16*, 1151−1170.
(22) Li, L.; Sun, J.; Li, X.; Zhang, Y.; Wang, Z.; Wang, C.; Dai, J.; Wang, Q. *Biomaterials* **2011**, *33*, 1714−1721.
(23) Zeng, J.; Xu, X.; Chen, X.; Liang, Q.; Bian, X.; Yang, L.; Jing, X. *J. Controlled Release* **2003**, *92*, 227−231.
(24) Reneker, D. H.; Yarin, A. L. *Polymer* **2008**, *49*, 2387−2425.
(25) Lansdown, A. *J. Wound Care* **2002**, *11*, 125−130.
(26) Shetty Akhila, J.; Deepa, S.; Alwar, M. *Curr. Sci.* **2007**, *93*, 917−920.
(27) Wang, J.; Zhou, G.; Chen, C.; Yu, H.; Wang, T.; Ma, Y.; Jia, G.; Gao, Y.; Li, B.; Sun, J. *Toxicol. Lett.* **2007**, *168*, 176−185.
(28) Chen, J.; Dong, X.; Zhao, J.; Tang, G. *J. Appl. Toxicol.* **2009**, *29*, 330−337. <!——>